Cucurbit[8]uril-derived graphene hydrogels

Vijay K. Rana,[†] Anthony Tabet,[†,‡] Julian A. Vigil,[†] Christopher J. Balzer,[†] Aurimas Narkevicius,[†] John Finlay,[‡] Clement Hallou,[‡] David H. Rowitch,[‡] Harry Bulstrode,[‡] and Oren A. Scherman*[,†]

†*Melville Laboratory for Polymer Synthesis, Department of Chemistry, University of Cambridge, Cambridge CB2 1EW, UK*

‡*Department of Paediatrics, Addenbrooke's Hospital, University of Cambridge, Hills Road, Cambridge CB2 0QQ, UK*

Received November 20, 2019; E-mail: oas23@cam.ac.uk

Abstract: The scalable production of uniformly distributed graphene (GR)-based composite materials remains a sizable challenge. While GR-polymer nanocomposites can be manufactured at large scale, processing limitations result in poor control over the homogeneity of hydrophobic GR sheets in the matrices. Such processes often result in difficulties controlling stability and avoiding aggregation, therefore eliminating benefits that might have otherwise arisen from the nanoscopic dimensions of GR. Here, we report an exfoliated and stabilized GR dispersion in water. Cucurbit[8]uril (CB[8])-mediated host-guest chemistry was used to obtain supramolecular hydrogels consisting of uniformly distributed GR and guest-functionalized macromolecules. The obtained GR-hydrogels show superior bioelectrical properties over identical systems produced without CB[8]. Utilizing such supramolecular interactions with biologically-derived macromolecules is a promising approach to stabilize graphene in water and avoid oxidative chemistry.

Graphene (GR) sheets are hydrophobic monolayers of sp^2 carbon atoms and are the thinnest known 2D material. GR based materials have been used in applications ranging from electronics and robotics to aviation and sports equipment.[1,2] Once GR is incorporated into polymer matrices, the resultant composites show enhanced mechanical, thermal, electrical and biological properties.[3,4] However, the low-cost production of uniformly distributed GR-based composite materials remains a sizable challenge.[5,6] For instance, GR-polymer nanocomposites can be manufactured at large scale, but processing limitations result in poor control over the homogeneity of GR sheets in the matrices. Such processes often cause difficulties in controlling stability and avoiding aggregation, therefore eliminating benefits that might have otherwise arisen from the nanoscopic dimensions of GR.[7–9] Substantial efforts are now being made to either chemically modify the surface of GR or impart stability *via* network-inducing groups, or use surfactants to improve their solubility and processability.

Oxidation of GR into graphene oxide (GO) is a popular approach to include and stabilize (reduced) GO sheets into matrices.[10] The presence of hydroxy, epoxy, carboxylic and other carbonyl-containing surface functional groups improves the solubility of GO in aqueous solutions, and allows robust crosslinking to form covalent networks of GO with polymers.[11] However, the production of GO requires strong oxidation conditions that disrupt many useful intrinsic properties of GR, including its superb conductivity. An alternative approach to form stabilized GR in water is to use small molecule surfactant-assisted exfoliation of graphite, a top down approach.[12–14] Small molecules such as pyrene and derivatives[8] are often used as surfactants to stabilize the exfoliated GR in water and organic solvents *via* supramolecular interactions. However, their toxicities present safety and scale-up concerns.[7]

The use of supramolecular interactions can impart many advantages over covalent networks in materials science.[15,16] We hypothesize that once exfolited GR is produced, larger molecules like polymers (matrices) can be employed to stabilized GR into matrices by forming supramolecular networks *via* host-guest interactions. Such interaction can take place between a surfactant (used for exfoliation) and a polymer itself. This can subsequently improve the properties of GR-polymer composites. Moreover, this approach exploits the advantages of supramolecular networks while potentially overcoming challenges that occur with both chemical functionalization and toxic surfactants.

In this work, cucurbit[8]uril (CB[8])-mediated host-guest complexation results in stabilization and reinforcement of exfoliated GR sheets by forming non-covalent supramolecular GR-hydrogels with guest functionalized polymers. Cucurbiturils (CB[n]s) are a symmetric class of macrocycles with many advantages over other macrocyclic hosts such as cyclodextrins and calixarene. Typically, CB[n]s have higher binding affinity than other macrocyclic hosts.[17] CB[8] can form 2:1 homoternary and 1:1:1 heteroternary complexes in water, and this property has been exploited to form hydrogels for drug delivery and other supramolecular structures for different applications.[17] Cyclodextrins have been previously used to stabilize graphene oxide and form hybrid materials for various applications.[18,19] Kumar and colleagues recently reported on CB[8]-mediated complexation of GO with other 2D materials *via* host-guest complexation.[20] The combination of GO and CB[7] has also been used for sensing applications.[21,22] Nevertheless, no studies to date have explored the utility of cucurbiturils in GR-based supramolecular hydrogels. Furthermore, all studies utilizing any macrocyclic host have focused mainly on GO, not GR and/or exfoliated GR, and have mostly required non-ambient conditions. Herein, self-assembled and CB[8]-mediated supramolecular GR-hydrogels are reported for the first time.

A silane-terminated viologen (MV^{2+}-silane) is used to exfoliate graphite into GR nanosheets (Fig. 1A, see ESI for details). Importantly, after exfoliation, the whole solution is dialyzed for 9 d to remove any unreacted MV^{2+}-silane molecules (Fig. S2). During exfoliation, MV^{2+} is covalently tethered to both sides of GR which improves the perco-

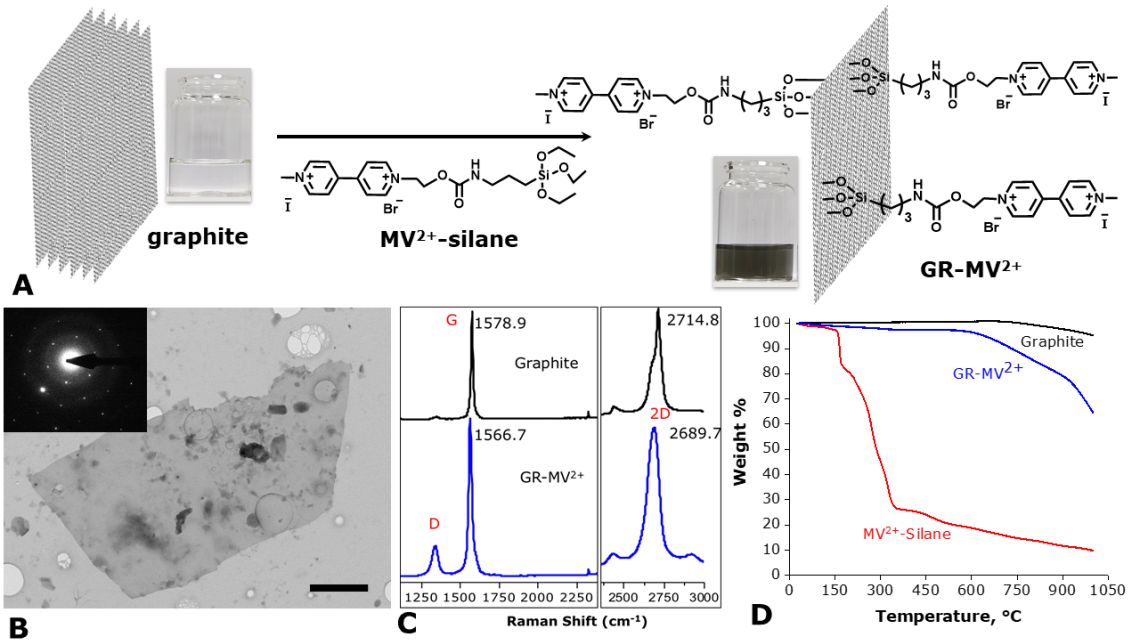

Figure 1. Synthesis and characterization of functional GR nanosheets. (A) MV^{2+}-silane assisted exfoliation of graphite into graphene, (B) TEM image of GR sheet of GR-MV^{2+} and inset selected area electron diffraction (SAED). Scale bar 1 μm. (C) Raman spectra of graphite and GR-MV^{2+}, (D) TGA thermograms of GR-MV^{2+}, MV^{2+}-silane and graphite.

lation of a 3D supramolecular network when mixed with guest-functionalized polymer and CB[8] (Fig. 2). MV^{2+} is a good first guest for CB[8]. After its complexation in the macrocycle's cavity a second guest can bind to form a 1:1:1 heteroternary complex.[17] Transmission electron microscopy (TEM) was first used to investigate GR-MV^{2+} morphology (Fig. 1B). The TEM data suggest that the sheets are large ($\sim$11.25 μm^2) and exist as a few layers. The selected area electron diffraction (SAED) displayed in the inset of Fig. 1B exhibits the typical hexagonal crystalline structure of GR. The spots related to the {1100} plane have higher intensities than those of the {2110} plane, indicating GR exists as non-agglomerated layers (Fig. S3).[23] Atomic force microscopy (AFM) was further employed to measure the thickness of the exfoliated sheets. After the height profile analysis, we found that the thickness of GR-MV^{2+} sheets is 1.2 nm (Fig. S4). This shows that between 3 and 5 sheets are stacked together in an exfoliated solution.

Raman data (Fig. 1C) shows the spectra of graphite and drop-cast GR-MV^{2+}. The strong G (1566.7 cm^{-1}) and 2D (2689.7 cm^{-1}) bands confirm that the GR-MV^{2+} has minimal sheet stacking. The upshifted 2D band (by 25.1 cm^{-1}) further supports that graphite was exfoliated into GR in solution.[24] Existence of a weak D band in the GR-MV^{2+} spectrum indicates that sonication has partially oxidized the GR-nanosheets introducing some defect sites. Such defects could be critical for the silane moieties of MV^{2+}-silane to covalently attach onto the GR surface.[23,25]

Thermogravimetric analysis (TGA) depicts nearly no weight loss for graphite up to 800 °C, whereas MV^{2+}-silane started to melt at 150 °C and decomposed completely by 550 °C (Fig. 1D). Interestingly, dialyzed and dried GR-MV^{2+} behaved differently and lost only $\sim$1.8 wt% between 150 °C to 550 °C. This could be due to the decomposition of attached MV^{2+} groups on the surface of GR.

X-ray photoelectron spectroscopy (XPS)survey spectra of graphite and GR-MV^{2+} is given in supporting information (Fig. S5). Graphite has two elements predominantly carbon (C1s, $\sim$99%) binding energy (BE) peak at 284.5 eV and oxygen (O1s, $\sim$1%) BE at 532.9 eV, whereas, GR-MV^{2+} has C1s ($\sim$92% at 284 eV), O1s ($\sim$4% at 532 eV), N1s ($\sim$2% at 399.5 eV), Si2p ($\sim$1% at 101.7 eV), and halides ($\sim$1%) elements. Higher percentage of O1s in GR-MV^{2+} than graphite confirms that the exfoliation has induced defects and partially oxidized the graphene. Moreover, presence of N1s and Si2p peaks only in GR-MV^{2+} confirms the fact that MV^{2+}-silane is present on the surface of exfoliated GR. The narrow N1s spectra of GR-MV^{2+} depicts two different nitrogen species one at BE at 401.5 eV is from viologen moiety and another one at 399.6 eV is from amide moiety of MV^{2+}-silane molecule (Fig. 6c). On the other hand, the narrow Si2p spectra also depicts two silane species (Fig. 6d). The first one at a BE of 102 eV represents the bond of silicon with oxygen originating from the GR, (-Si-O-GR), the second one at 102.7 eV is apparently attributed to the siloxane (-Si-O-Si-), resulting from the partial hydrolysis of MV^{2+}-silane molecules during the silanization reaction on the GR surface.[26]

The attenuated total reflection Fourier-transform infrared spectroscopy (ATR-FTIR) spectrum of GR-MV^{2+} illustrates the combination of peaks in the range of 1091 to 798 cm^{-1} correspond to -C-Si-O- and -Si-O-Si- bands (see Fig. S7). The peak at 1630 cm^{-1} relates to the carbonyl groups and the broad peaks at 3333 and 3190 cm^{-1} correspond to the hydroxyl and amine groups of GR-MV^{2+}, respectively. The IR spectrum of graphite does not contain any of these absorbance peaks, whereas MV^{2+}-silane shows all the peaks for viologen and silane moieties. The solution phase ^1H NMR confirms that the characteristic peaks of α and β protons of MV^{2+}-$CH_2CH_2OCONHCH_2\boldsymbol{CH_2CH_2}SiO_3R$- were broadened and shifted upfield when MV^{2+}-silane was sonicated with graphite for 9 h (see Fig. S8). Energy-dispersive spectroscopy (EDS) mapping and elemental analysis of graphite

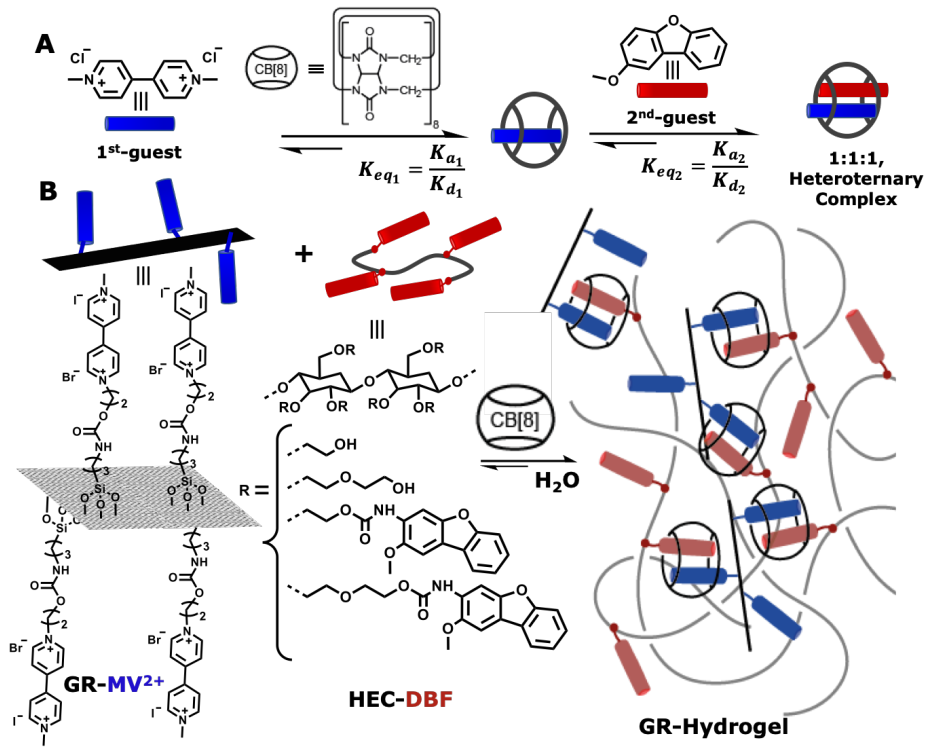

Figure 2. Illustration of dynamic supramolecular interactions. (A) Schematic illustration of the two-step binding of CB[8] with first-guest (methyl viologen, MV^{2+}) and second-guest (dibenzofuran, DBF). (B) Supramolecular hydrogel formed after the non-covalent host-guest interactions between GR-MV^{2+}, HEC-DBF, and CB[8].

and GR-MV^{2+} revealed that the silicon atom peak (2.6 wt%) of MV^{2+}-silane was only present on the surface of GR-MV^{2+} (Fig. S9). These data together strongly indicate that GR nanosheets were surface-functionalized with the hydrophilic CB[8] guest MV^{2+}.

The electrostatic repulsion originating from hydrophilic dicationic viologens present on the surface of GR sheets dramatically improves their solubility in aqueous solutions (Fig 1A). Such amphiphilic systems were stable for at least 6 months in solution. When cucurbit[7]uril (CB[7]) or CB[8], which can both form 1:1 complexes with MV^{2+}, were introduced into the dispersions, no visible change in their stability was observed. However, the stability was improved when the second guest-functionalized polymer hydroxyethyl cellulose-dibenzofuran (HEC-DBF) was introduced to the GR solution with CB[8]. MV^{2+} and DBF can form a 1:1:1 heteroternary complex with CB[8] (Fig. 2), but not with CB[7]. The formation of a supramolecular hydrogel ($G' > G''$) was observed when CB[8] was present in the system with 1.25 wt% HEC-DBF and 0.0125 wt% GR-MV^{2+} (Fig. 2B), whereas the solution formed a viscous liquid ($G' < G''$) with CB[7] or without any CB (Fig. 3E-G and Fig. S10). Fig. 3A shows that the gel with CB[8] did not flow under gravity whereas the viscous solutions with no CB or with CB[7] did. An oscillatory frequency sweep of this gel shows its dynamic moduli G' is 158 Pa at 1 rad/s (Fig. 3G). GR-MV^{2+} solutions with HEC-DBF and CB[7] or without any CB were not stable after 7 d suggesting the high molecular weight polysaccharide can disrupt the repulsion between GR-MV^{2+} sheets (Fig. S11). The GR-hydrogel was further analyzed using scanning electron microscopy (SEM) and transmission electron microscopy (TEM). SEM images (Fig.3B-D, and S12) of the freeze-dried gel show a porous network. TEM analysis was carried out after diluting hydrogels in water and a solution was mounted on a TEM grid. The obtained TEM images (Fig.3C-D,) suggest the existence of both polymer (organic, dashed line) and GR sheets (arrow) in GR-hydrogels.

We next characterized the phase behavior of these CB[8] hydrogels more rigorously (Fig. 3H-I). We first identified the percolation threshold of the gel when the concentration of CB[8] was varied (Fig. 3H). We found that the sol-gel transition occurs when 0.2 molecules of CB[8] are added for every molecule of 2nd guest. Additionally, the stiffness plateaued at 1 CB[8] molecule per 2nd guest, which was expected as network formation is contingent on 1:1:1 host-guest complexation. We also varied the total gel weight fraction and found the sol-gel transition to occur between 1.2 and 1.3% wt/wt. Taken together, these two phase diagrams confirm that CB[8] mediates the formation of GR hydrogels and the total weight fraction required for gelation is comparable to other supramolecular hydrogels.[27,28]

Gelation and subsequent stability of the GR-MV^{2+}/HEC-DBF system occur due to 1:1:1 complexation with CB[8]. MV^{2+} can be readily reduced to $MV^{+\bullet}$ with $Na_2S_2O_4$, and these $MV^{+\bullet}$ species form 2:1 homoternary complexes with CB[8].[17] Upon addition of $Na_2S_2O_4$ into GR-MV^{2+}/CB[8] solutions, the graphene sheets aggregated (<30 min, Fig. S13), whereas in the absence of CB, or in the presence of CB[7] the solution remained unchanged over the same time frame. Furthermore we also screened a library of MV^{2+} derivatives, including silanol-terminated viologen, as well as second guest surfactants to exfoliate graphite into GR. MV^{2+}-silane outperformed all these systems, suggesting possible covalent tethering of silane moieties to the partially oxidized GR sheets (defects arising from sonication) that improves aqueous stability of GR (Fig. S14 & S15) and eventually participates in supramolecular host-guest inter-

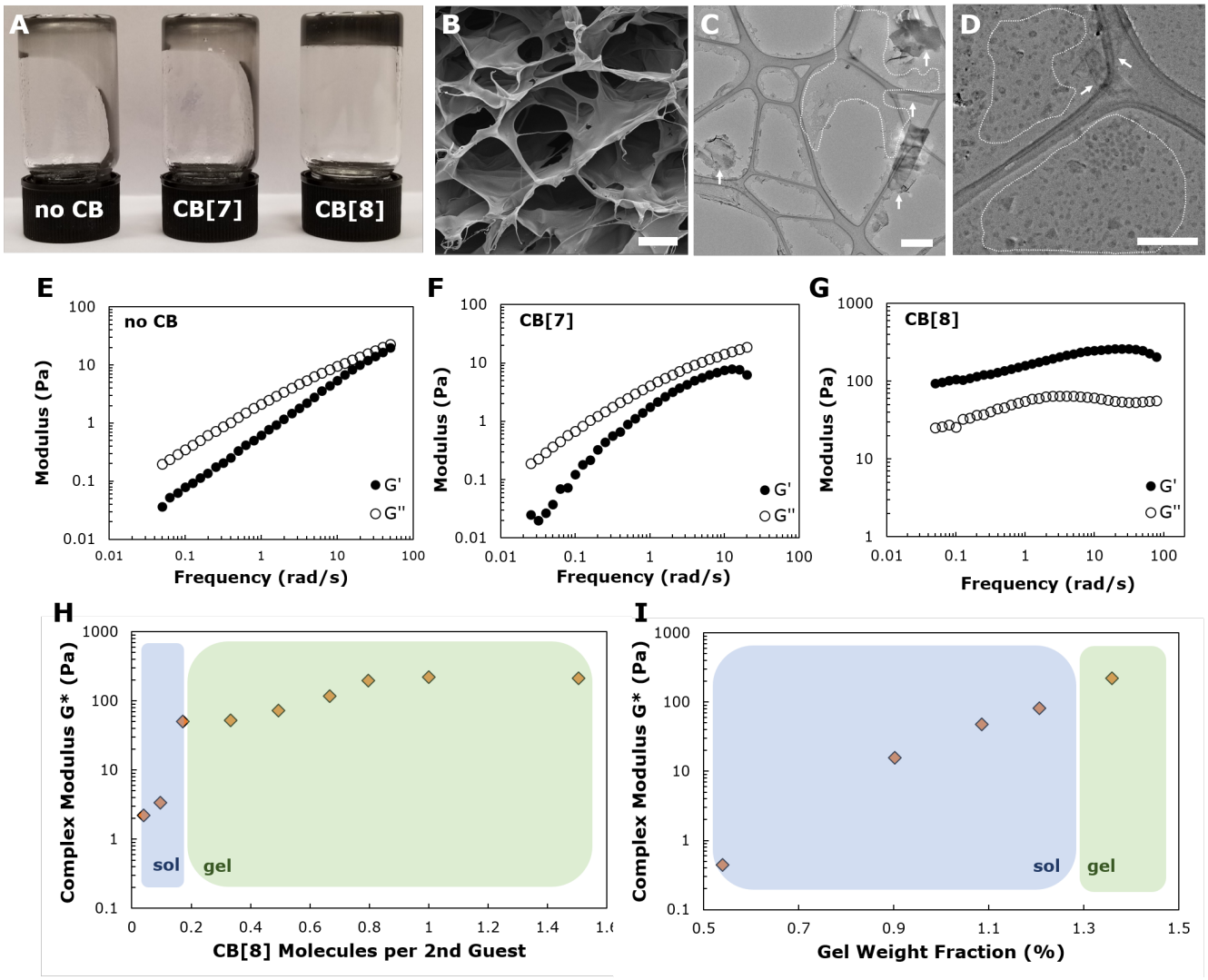

Figure 3. Characterization of the supramolecular hydrogel. (A) Image of GR-MV^{2+} and HEC-DBF composite without CB, with CB[7], and with CB[8]. Inverted-vials demonstrate that only CB[8]-based systems (1.25 wt% HEC-DBF and 0.01 wt% GR-MV^{2+}) formed gels. (B-D) Micrographs of the CB[8]-mediated GR-hydrogel. (B) SEM and (C-D) TEM images of the diluted gel. Dotted lines cover the organic sections and arrows indicate the presence of GR sheets. Scale bars: (B) 10 micron, (C) 1 micron, (D) 500 nm. (E-G) Oscillatory frequency sweeps of (E) no CB, (F) CB[7], and (G) CB[8] systems plotting G′ and G″ against frequency at 20 °C in the linear viscoelastic region. (H) Phase diagram showing the sol-gel transition as a function of the number of CB[8] molecules relative to 2nd guest molecules. Complex modulus is plotted against CB[8] ratio at 1 rad/s. The sol-gel transition occurs between 0.1 and 0.2 CB[8] molecules per 2nd guest. Saturation occurred at 1 CB[8] molecule per 2nd guest. (I) Phase diagram showing the sol-gel transition as a function of total network weight fraction. Complex modulus is plotted against weight fraction at 1 rad/s. The sol-gel transition occurs between 1.2 and 1.3%.

actions.

The conductive properties of the GR-MV^{2+}/HEC-DBF systems were explored with potentiostatic electrochemical impedance spectroscopy (PEIS). Systems with CB[8] were more conductive than those without CB or those with CB[7] (Fig. S16, S17A). Improved GR-dispersion and CB[8]-mediated charge transfer interactions between MV^{2+} and DBF likely complemented the ionic diffusion-based conductivity present in the graphene gel systems. Surprisingly, the system with CB[7] was more conductive than those without any CB, but notably less than CB[8].

Finally, the cytotoxicity of these systems was explored with adult mouse neural stem cells (Fig. S17B-C). While GR alone has been reported as non-cytotoxic,[29] the toxicity of MV^{2+} is well documented. Binding suchs guests to CB[7] and CB[8] is one strategy to reduce their toxicity.[17] When GR-MV^{2+}/HEC-DBF systems were coincubated with the neural stem cells at 100 μg/mL, CB[8] capped systems showed no acute adverse toxicity, whereas this was not the case for the system without any CB or for the system containing CB[7]. The latter is likely a result of DBF that may trigger adverse effects.[30] The concentrations where cell compatibility was observed are relatively low, which limits these gels' utility for parenteral drug delivery.[31] Applications such as gene delivery[32] or as part of a composite for the co-delivery of hydrophobic small molecule drugs are more promising. Overall, the conductivity and acute cytotoxity of GR-hydrogels were improved. Rhodamine B was used to show that water-soluble small molecules do not crash out despite the presence of hydrophobic components (Fig. S13). This confirms our hypothesis that once exfoliated GR is produced, larger molecules like polymers (HEC) can be used to stabilize GR into matrices by forming supramolecular networks *via* host-guest interactions and improve properties.

This report demonstrates the first synthesis of CB[8]-mediated graphene hydrogels. Host-guest complexation of MV^{2+} guests attached to GR sheets and DBF on the backbone of HEC with CB[8] drove network formation. Characterization techniques confirmed that exfolited-GR sheets were surface-functionalized with MV^{2+}. CB[8] was required to form a supramolecular hydrogel and improve the electrical and biological properties of the system over equivalent systems in the absence of CBs or in the presence of CB[7]. These experiments both highlight the value of dicationic viologens in exfoliating GR sheets in water, which can be made biologically inert through complexation with CB[8], and the role that supramolecular chemistry and macrocyclic hosts can play in improving electro-physiological properties of GR sheets in a polymeric matrix.

Acknowledgement V.K.R. thanks the Marie Sklodowska-Curie individual research grant (H2020-MSCA-IF-2017, P.ID: 797106) for funding support. A.T., J.A.V., C.J.B., and J.F. thank The Winston Churchill Foundation of the United States for funding support. A.N. thanks EPSRC Doctoral Training Grant EP/N509620/1. O.A.S. acknowledges EPSRC Programme Grant NOtCH (EP/L027151/1) for financial support. We thank Dr. Kamil Sokolowski for his help with ^{1}H NMR titrations and Cyan Williams and Yu Ogawa for their support in sonication and SEAD measurments, respectively. We also thank Dr. Stefan Mommer for illustrative support.

Associated Content The Supporting Information contains NMR, rheology, TEM, AFM, XPS, ATR-FTIR, EDS, SEM, impedance, and cell confluence data.

References

(1) Zhu, Y.; Murali, S.; Cai, W.; Li, X.; Suk, J. W.; Potts, J. R.; Ruoff, R. S. Graphene and graphene oxide: Synthesis, properties, and applications. *Adv. Mater.* **2010**, *22*, 3906–3924.
(2) Cheng, C.; Li, S.; Thomas, A.; Kotov, N. A.; Haag, R. Functional Graphene Nanomaterials Based Architectures: Biointeractions, Fabrications, and Emerging Biological Applications. *Chem. Rev.* **2017**, *117*, 1826–1914.
(3) Ramanathan, T.; Abdala, A. A.; Stankovich, S.; Dikin, D. A.; Herrera-Alonso, M.; Piner, R. D.; Adamson, D. H.; Schniepp, H. C.; Chen, X.; Ruoff, R. S.; Nguyen, S. T.; Aksay, I. A.; Prud'homme, R. K.; Brinson, L. C. Functionalized graphene sheets for polymer nanocomposites. *Nat. Nanotechnol.* **2008**, *3*, 327–331.
(4) Stankovich, S.; Dikin, D. A.; Dommett, G. H.; Kohlhaas, K. M.; Zimney, E. J.; Stach, E. A.; Piner, R. D.; Nguyen, S. B. T.; Ruoff, R. S. Graphene-based composite materials. *Nature* **2006**, *442*, 282–286.
(5) Kuila, T.; Bhadra, S.; Yao, D. H.; Kim, N. H.; Bose, S.; Lee, J. H. Recent advances in graphene based polymer composites. *Prog. Polym. Sci.* **2010**, *35*, 1350–1375.
(6) Johnson, D. W.; Dobson, B. P.; Coleman, K. S. A manufacturing perspective on graphene dispersions. *Curr. Opin. Colloid Interface Sci.* **2015**, *20*, 367–382.
(7) Georgakilas, V.; Tiwari, J. N.; Kemp, K. C.; Perman, J. A.; Bourlinos, A. B.; Kim, K. S.; Zboril, R. Noncovalent Functionalization of Graphene and Graphene Oxide for Energy Materials, Biosensing, Catalytic, and Biomedical Applications. *Chem. Rev.* **2016**, *116*, 5464–5519.
(8) Ciesielski, A.; Samorì, P. Graphene via sonication assisted liquid-phase exfoliation. *Chem. Soc. Rev.* **2014**, *43*, 381–398.
(9) Carey, T.; Cacovich, S.; Divitini, G.; Ren, J.; Mansouri, A.; Kim, J. M.; Wang, C.; Ducati, C.; Sordan, R.; Torrisi, F. Fully inkjet-printed two-dimensional material field-effect heterojunctions for wearable and textile electronics. *Nat. Commun.* **2017**, *8*, 1202.
(10) Dreyer, D. R.; Park, S.; Bielawski, C. W.; Ruoff, R. S. Graphite oxide. *Chem. Soc. Rev.* **2010**, *39*, 228–240.
(11) Chee, W. K.; Lim, H. N.; Huang, N. M.; Harrison, I. Nanocomposites of graphene/polymers: a review. *RSC Adv.* **2015**, *5*, 68014–68051.
(12) Li, D.; Müller, M. B.; Gilje, S.; Kaner, R. B.; Wallace, G. G. Processable aqueous dispersions of graphene nanosheets. *Nat. Nanotechnol.* **2008**, *3*, 101–105.
(13) Chabot, V.; Kim, B.; Sloper, B.; Tzoganakis, C.; Yu, A. High yield production and purification of few layer graphene by Gum Arabic assisted physical sonication. *Sci. Rep.* **2013**, *3*, 1378.
(14) Nicolosi, V.; Chhowalla, M.; Kanatzidis, M. G.; Strano, M. S.; Coleman, J. N. Liquid Exfoliation of Layered Materials. *Science* **2013**, *340*.
(15) Webber, M. J.; Appel, E. A.; Meijer, E. W.; Langer, R. Supramolecular biomaterials. *Nat. Mater.* **2015**, *15*, 13–26.
(16) Dubbin, K.; Tabet, A.; Heilshorn, S. C. Quantitative criteria to benchmark new and existing bio-inks for cell compatibility. *Biofabrication* **2017**, *9*.
(17) Barrow, S. J.; Kasera, S.; Rowland, M. J.; Del Barrio, J.; Scherman, O. A. Cucurbituril-Based Molecular Recognition. *Chem. Rev.* **2015**, *115*, 12320–12406.
(18) Guo, Y.; Guo, S.; Ren, J.; Zhai, Y.; Dong, S.; Wang, E. Cyclodextrin functionalized graphene nanosheets with high supramolecular recognition capability: Synthesis and host - Guest inclusion for enhanced electrochemical performance. *ACS Nano* **2010**, *4*, 4001–4010.
(19) Konkena, B.; Vasudevan, S. Covalently linked, water-dispersible, cyclodextrin: Reduced-graphene oxide sheets. *Langmuir* **2012**, *28*, 12432–12437.
(20) Kumar, R.; Jalani, K.; George, S. J.; Rao, C. N. Non-Covalent Synthesis as a New Strategy for Generating Supramolecular Layered Heterostructures. *Chem. Mater.* **2017**, *29*, 9751–9757.
(21) Wei, T.; Dong, T.; Xing, H.; Liu, Y.; Dai, Z. Cucurbituril and Azide Cofunctionalized Graphene Oxide for Ultrasensitive Electro-Click Biosensing. *Anal. Chem.* **2017**, *89*, 12237–12243.
(22) Prakash, R.; Usha, G.; Sivaranjana, P.; Karpagalakshmi, K.; Piramuthu, L.; Selvapalam, N. Graphene oxide based fluorescence sensor for cucurbit[7]uril. *New J. Chem.* **2018**, *42*, 13038–13043.
(23) Xu, H.; Suslick, K. S. Sonochemical preparation of functionalized graphenes. *J. Am. Chem. Soc.* **2011**, *133*, 9148–9151.
(24) Ferrari, A. C. Raman spectroscopy of graphene and graphite: Disorder, electron-phonon coupling, doping and nonadiabatic effects. *Solid State Commun.* **2007**, *143*, 47–57.
(25) Skaltsas, T.; Ke, X.; Bittencourt, C.; Tagmatarchis, N. Ultrasonication induces oxygenated species and defects onto exfoliated graphene. *J. Phys. Chem. C* **2013**, *117*, 23272–23278.
(26) Ma, P. C.; Kim, J. K.; Tang, B. Z. Functionalization of carbon nanotubes using a silane coupling agent. *Carbon* **2006**, *44*, 3232–3238.
(27) Tabet, A.; Forster, R. A.; Parkins, C. C.; Wu, G.; Scherman, O. A. Modulating stiffness with photo-switchable supramolecular hydrogels. *Polymer Chemistry* **2019**,
(28) Tabet, A.; Mommer, S.; Vigil, J. A.; Hallou, C.; Bulstrode, H.; Scherman, O. A. Mechanical Characterization of Human Brain Tissue and Soft Dynamic Gels Exhibiting Electromechanical Neuro-Mimicry. *Advanced Healthcare Materials* **2019**,
(29) Bianco, A. Graphene: Safe or toxic? the two faces of the medal. *Angew. Chemie. Int. Ed.* **2013**, *52*, 4986–4997.
(30) Arulmozhiraja, S.; Morita, M. Structure-Activity Relationships for the Toxicity of Polychlorinated Dibenzofurans: Approach through Density Functional Theory-Based Descriptors. *Chem. Res. Toxicol.* **2004**, *17*, 348–356.
(31) Tabet, A.; Wang, C. . *Adv. Healthcare Mater.* **2018**, *1800908*.
(32) Lin, W.; Hanson, S.; Han, W.; Zhang, X.; Yao, N.; Li, H.; Zhang, L.; Wang, C. Well-defined star polymers for co-delivery of plasmid DNA and imiquimod to dendritic cells. *Acta Biomaterialia* **2017**, *48*, 378–389.

Graphical TOC Entry

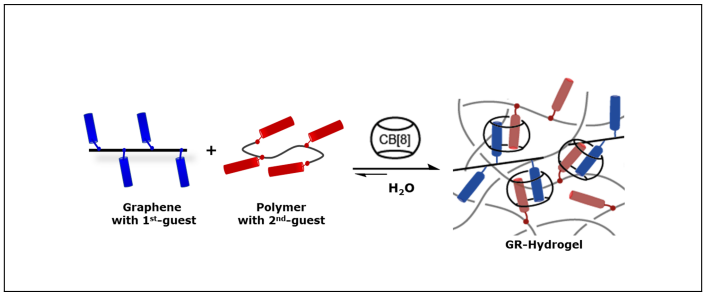

Supramolecular graphene hydrogels are reported. Exfoliated graphene nanosheets are stabilized in aqueous networks through supramolecular interactions with functionalized polymers and the macrocycle cucurbit[8]uril.